

Measuring muon neutrino disappearance
with the NOvA experiment

Luke Vinton

Declaration

I hereby declare that this thesis has not been and will not be submitted in whole or in part to another University for the award of any other degree.

Signature:

Luke Vinton

UNIVERSITY OF SUSSEX

LUKE VINTON, DOCTOR OF PHILOSOPHY

MEASURING MUON NEUTRINO DISAPPEARANCE WITH THE NOVA EXPERIMENT

SUMMARY

Abstract

Acknowledgements

Contents

List of Tables	vi
List of Figures	vii
1 Introduction	1
2 Neutrino Physics	2
2.1 The Standard Model	2
2.2 The Weak Force	2
2.3 Neutrino Oscillations	2
2.4 Need to include the following	3
3 The NOvA Experiment	4
3.1 The NuMI Beam	4
3.1.1 Off-axis Detectors	5
3.1.2 Horn Position	8
3.2 The NOvA Detectors	8
3.2.1 The Basic NOvA Detector Element	8
3.2.2 Liquid Scintillator	9
3.2.3 Detector Assembly	9
3.2.4 Data Aquisition	9
3.2.5 The Far Detector	9
3.2.6 The Near Detector	9
4 Energy Resolution	11
Bibliography	12

List of Tables

List of Figures

3.1	A diagram showing the layout of the NuMI beam.	5
3.2	The above distributions are as viewed from a site located 800km from the NuMI target and off-axis by an angle θ	6
3.3	Charged current ν_μ event rates vs. neutrino energy in the absense of oscillations. The distributions are found for a detector which is 800 km from the NuMI target and for various off-axis angles.	7
3.4	Simulated visible energy distributions for ν_μ CC events with and without oscillations, ν_e oscillation signal events, intrinsic beam ν_e events and neutral current events. The simulation assumes an off-axis position of 12 km at 810 km, $\Delta m^2 = 2.5 \times 10^{-3} \text{eV}^2$, $\sin^2(2\theta_{23}) = 1.0$ and $\sin^2(2\theta_{13}) = 0.1$	7
3.5	Liquid scintillator composition. cite	9
3.6	A NOvA cell consisting of an extruded PVC tube filled with liquid scintillator and a looped WLS fibre.	10
3.7	A side on view of a module constructed from 18 cells glued together.	10
3.8	Cut out of a NOvA detector showing the alternating orientation of the stacked planes.	10

Chapter 1

Introduction

Chapter 2

Neutrino Physics

2.1 The Standard Model

Our current understanding of particle physics is well described by the Standard model, which describes the interactions between fundamental particles and the weak, electromagnetic and strong forces.

2.2 The Weak Force

Neutrinos interact with matter through the weak force in one of three flavour eigenstates (electron, muon or tau). The weak force is mediated by the electrically charged W^\pm and electrically neutral Z bosons.

Include feynam diagrams of the neutrino interactions.

A neutrino interacting with matter through the W boson will produce a charged lepton corresponding to the weak flavour of the incoming neutrino. This process can happen in reverse, with a charged lepton producing a neutrino with the same flavour and a W boson. Such processes involving a W boson are known as charged current interactions (CC interactions).

2.3 Neutrino Oscillations

As current understanding has it, neutrinos come in three eigenstates of the weak force (electron, muon and tau) and three mass eigenstates (m_1 , m_2 or m_3). The weak eigenstates do not correspond directly to the mass eigenstates. Instead, the weak eigenstates are a superposition of the mass states and vice versa.

Once produced, neutrinos propagate as a superposition of mass eigenstates

2.4 Need to include the following

Meson decay for neutrino beam production

Chapter 3

The NOvA Experiment

The NOvA experiment (NuMI Off-axis ν_e Appearance) consists of two detectors which measure the neutrino composition of the NuMI (Neutrinos at the Main Injector). The 300 ton near detector is on site at Fermilab and is located 1.015 km from the NuMI target hall. The 14 kiloton far detector is located 810km from the NuMI target hall. Both detectors are placed off-axis from the centre of the NuMI beam by 14.6 mrad.

The original design of the NOvA experiment is laid out in the technical design report (TDR) [1]. The constructed experiment differs only slightly with the design laid out in the TDR. The details of the constructed experiment, including the neutrino beam source and the two detectors, are discussed in the following chapter.

3.1 The NuMI Beam

The NOvA experiment's neutrino source is provided by the Neutrinos at the Main Injector (NuMI) beam at Fermilab. The following section describes the process by which the NuMI muon neutrino beam is created.

An instructive diagram of the NuMI beam is presented in Figure 3.1. The Main Injector accepts six batches, each spanning 10 μ sec, of protons at a time and accelerates the protons up to 120 GeV. The accelerated protons are directed to collide with a 95cm long graphite target. The collision protons with the carbon atoms of the target produce a plethora of mesons (mostly pions and kaons). The charged mesons are focused into a beam by two magnetic focussing horns. The focussing horns are run in Forward Horn Current (FHC) or Reverse Horn Current (RHC) mode to select positively or negatively charged mesons respectively, leading to a neutrino or an anti-neutrino beam respectively.

The focussed beam of charged mesons then travels through a 675 m long evacuated

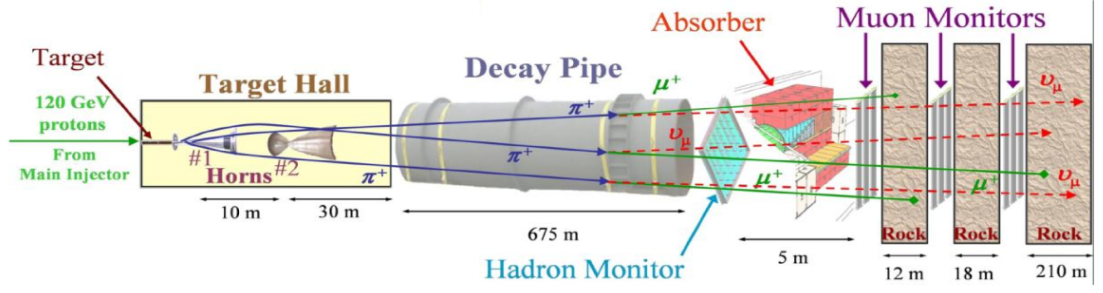


Figure 3.1: A diagram showing the layout of the NuMI beam.

decay pipe. Along this length of pipe the mesons decay to charged leptons and neutrinos. The decay pipe is followed by hadron and muon monitors and about 240m of rock. The rock absorbs the remaining charged particles in the beam before reaching the near detector.

after main description talk about the beam upgrades: slip-stacking and power. water cooling

3.1.1 Off-axis Detectors

The NOvA detectors are both placed 14 mrad off the axis of the NuMI beam. The reasons for placing the detector will be described in more detail in the following paragraphs.

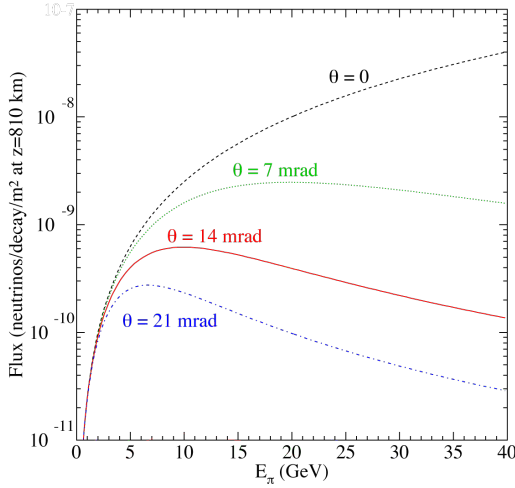
The decay used to produce a neutrino beam is a two body decay, where a pion (or kaon) decays to a neutrino and a muon. The two body decay occurs isotropically in the parent particles rest frame. In the lab frame the parent particle is not at rest when decaying. For pion and kaon decay this boosts the neutrinos into a cone in the direction of the parent particle. For small angles, the flux and energy of neutrinos produced by pion decay ($\pi \rightarrow \nu_\mu + \mu$) are given by:

$$\Phi = \left(\frac{2\gamma}{1 + \gamma^2\theta^2} \right)^2 \frac{A}{4\pi z^2} \quad (3.1)$$

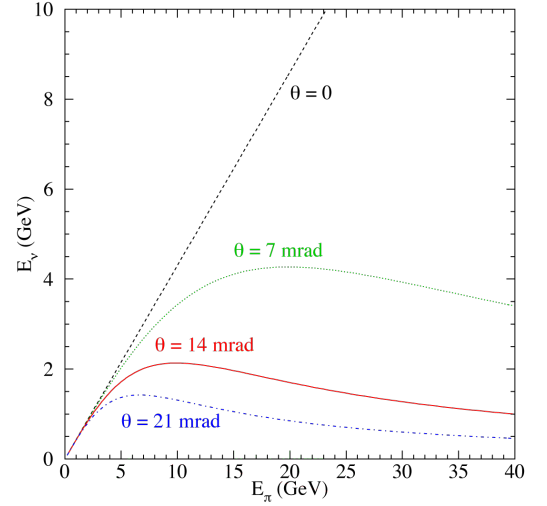
$$E_\nu = \frac{0.43E_\pi}{1 + \gamma^2\theta^2}, \quad (3.2)$$

where E_π is the energy of the parent pion, m_π the mass of the parent pion, θ the angle between the pion and neutrino directions and $\gamma = E_\pi/m_\pi$.

Equations 3.1 and 3.2 are shown as functions of neutrino energy and off-axis angle in Figure 3.2. Figure 3.3 shows the number of neutrino events as a function of the charged current ν_μ energy for the Low (left plot) and Medium (right plot) Energy Tune for various off-axis angles.



(a) Neutrino flux vs. pion energy.



(b) Neutrino energy vs. pion energy.

Figure 3.2: The above distributions are as viewed from a site located 800km from the NuMI target and off-axis by an angle θ .

For the Medium Energy Tune, figure 3.2b shows that at 14 mrad the neutrino energy does not have a strong dependence on the parent pion energy. In addition, figure 3.3b shows that at 14 mrad the Medium Energy Tune produces a narrow energy neutrino beam with approximately 4 times more neutrinos at 2GeV than the on-axis scenario. This peak at 2 GeV is well matched to the expected energy of the oscillation maximum. The oscillation maximum for electron neutrino appearance in a muon neutrino beam is expected to occur at 1.6 GeV for NOvA's L/E and for $\Delta m_{32}^2 = 2.4 \text{ meV}^2$.

As described above, placing the detector off-axis increases the flux at the expected oscillation maximum. In addition the narrow energy range of the off-axis beam improves the rejection of background events. Neutral current events are an important background source whose topologies can be hard to distinguish from electron showers produced by ν_e CC events. For NC events the neutrino carries a significant amount of the energy away and the visible energy tends to "feed down" to lower energies. For narrow band off-axis beam this feed down tends to shift the neutral current events to lower energies outside the ν_e appearance signal energy window. Figure 3.4 shows the number of ν_μ , ν_e and NC events as a function of visible energy, the bulk of the NC events (black histogram) are shown to shift below the signal region (red-hatched histogram).

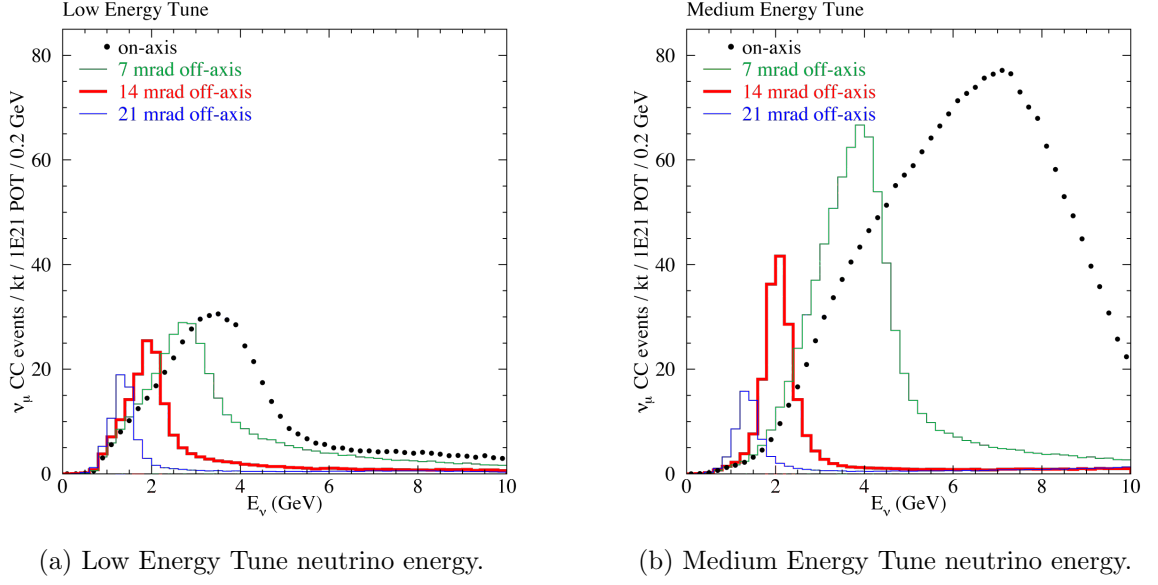


Figure 3.3: Charged current ν_μ event rates vs. neutrino energy in the absence of oscillations. The distributions are found for a detector which is 800 km from the NuMI target and for various off-axis angles.

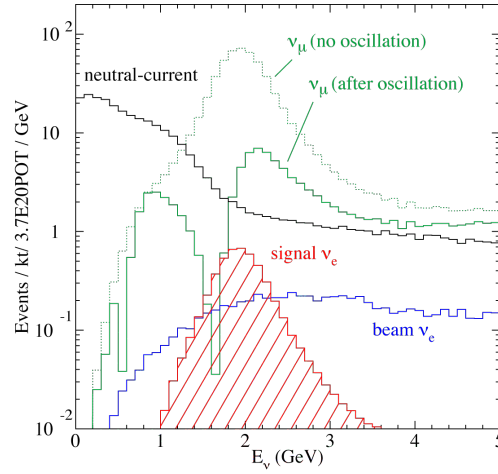


Figure 3.4: Simulated visible energy distributions for ν_μ CC events with and without oscillations, ν_e oscillation signal events, intrinsic beam ν_e events and neutral current events. The simulation assumes an off-axis position of 12 km at 810 km, $\Delta m^2 = 2.5 \times 10^{-3} \text{eV}^2$, $\sin^2(2\theta_{23}) = 1.0$ and $\sin^2(2\theta_{13}) = 0.1$.

3.1.2 Horn Position

3.2 The NOvA Detectors

The NOvA experiment uses a near and far detector to measure neutrino oscillations. The near detector is used to measure the unoscillated neutrino energy spectrum and the electron neutrino component of the beam. The unoscillated neutrino energy spectrum measured by the near detector is extrapolated to the far detector (**need to discuss further in a future chapter**). The far detectors purpose is to measure the energy spectrum of the beam neutrinos for comparison with the extropalted near detector energy spectrum.

The NOvA experiment aims to perform both $\nu\mu$ disappearance and νe appearance measurements. The detectors are designed to distinguish electron and muon neutrino charged current events from backgrounds.

The near and far NOvA detectors are almost functionally identical. Besides the different masses there are a few physical differences. The near detector has a so called “muon catcher”, has a higher rate of readout and uses slightly different APDs. The construction common among both detectors will be discussed in the following section. The details specific to the far and near detectors will be discussed in Subsections 3.2.5 and 3.2.6 respectively.

3.2.1 The Basic NOvA Detector Element

The basic unit of both NOvA detectors is a rectangular rigid PVC cell which contains liquid scintillator and a wavelength-shifting (WLS) fibre. An illustration of the cell is shown in Figure 3.6. The WLS fibre, which is twice the length of the cell, is looped at the bottom of the cell such that the captured light travels in two directions to the instrument top end of the cell. At the top end of the cell each end of the looped fibre is directed onto one pixel of an Avalanche Photo Diode (APD) array. The APD converts the light from the WLS to a digital signal.

The NOvA cells are made from highly reflective titanium dioxide loaded rigid PVC. The cells have 2 and 4.5 mm thick walls, an interior depth of 5.9 cm along the beam direction, an interior width of 3.8 cm transverse to the beam direction and an interior length of 15.5 m.



Figure 3.5: Liquid scintillator composition. cite

3.2.2 Liquid Scintillator

Approximately 70% of the NOvA detector mass is composed of the liquid scintillator within the cells. The composition of the liquid scintillator is shown in Figure 3.5.

In addition 4.1% pseudocumene as the scintillant.

3.2.3 Detector Assembly

The NOvA detectors are constructed using extruded PVC tubes. Each PVC tube is called a cell and is filled with liquid scintillator and a Wave Length Shifting (WLS) fibre (see Figure 3.6). 18 cells are glued together side by side to form a module (see Figure 3.7). Modules are then glued together, again side by side, to form a plane. The planes layered with alternating orthogonal orientations, such that the orientation of the cells making up the plain alternate between horizontal and vertical from plane to plane (see Figure 3.8). The orthogonal orientation of the planes allows for three dimensional reconstruction of tracks passing through multiple planes. Planes are glued together in the orthogonal arrangement described above to form one solid piece called a block. Blocks are placed one after another to form the physical detectors.

3.2.4 Data Acquisition

Follow from the WLS fibre to APD, to FEB and to DCM.

Explain digitisation via single and multi point readout.

3.2.5 The Far Detector

Detector on the surface. Overburden of gravel and barite.

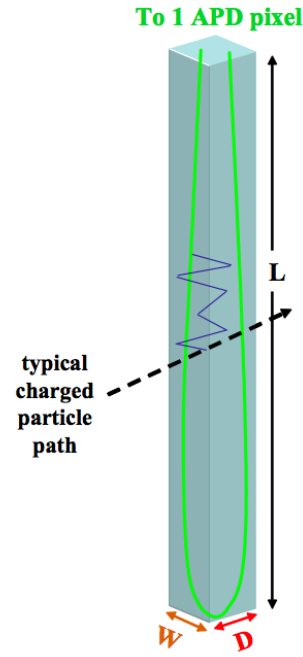


Figure 3.6: A NOvA cell consisting of an extruded PVC tube filled with liquid scintillator and a looped WLS fibre.

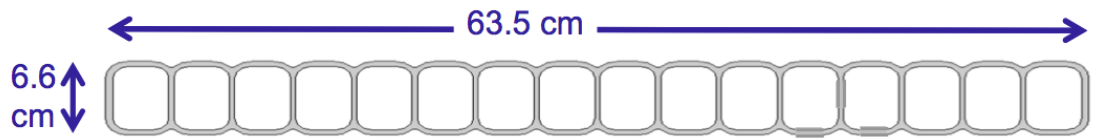


Figure 3.7: A side on view of a module constructed from 18 cells glued together.

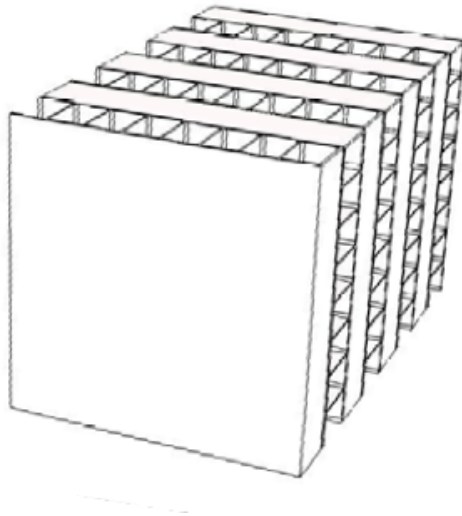


Figure 3.8: Cut out of a NOvA detector showing the alternating orientation of the stacked planes.

3.2.6 The Near Detector

Underground detector. Reduces cosmic ray background.

muon catcher. used to range out muons that would exit otherwise

older APDs. Something to do with the baked/non-baked

faster readout due to higher data rate near the neutrino source (higher flux)

Chapter 4

Energy Resolution

Energy resolution binning was implemented in MINOS to improve the sensitivity of the experiment. Techniques similar to those found in [\[2\]](#) will be used in the following chapter to improve the sensitivity of the NOvA experiment.

Bibliography

- [1] D. S. Ayres et al. The NOvA Technical Design Report. *Fermilab Publication*, 2007. [4](#)
- [2] John Stuart Marshall. *A study of muon neutrino disappearance with the MINOS detectors and the NuMI neutrino beam*. PhD thesis, Cambridge U., 2008. [11](#)